Vehicle Path Optimization for Angle-of-Arrival Localization

John McGuire*, Kutluyil Doğançay*, Yee Wei Law*, Javaan Chahl*†
*School of Engineering, University of South Australia, Mawson Lakes, SA 5095, Australia
†Joint and Operations Analysis Division, Defence Science and Technology Group, Melbourne, VIC 3207, Australia

***Abstract*—In this paper an optimal path planning algorithm is presented for a vehicle performing angle-of-arrival (AoA) self-localization. Noisy AoA measurements received from stationary beacons in the environment are used to estimate the position and heading of the vehicle. A gradient descent algorithm is presented to determine an optimal heading for a constant speed vehicle and a control input is calculated and implemented to achieve a desired trajectory. The platform path is optimized by minimizing a cost function derived from the mean-square error of predicted vehicle position produced by an extended Kalman filter. The vehicle trajectory must also satisfy position constraints, limiting the minimum distance between the platform and the transmitters. Simulations illustrate the effectiveness of the algorithm in environments with different beacon geometries and different initial estimate certainty.**

***Index Terms*—AoA localization, extended Kalman filter, optimal maneuvering.**

I. Introduction

Localization is an important capability for any autonomous system operating in an uncertain or unknown environment. For an autonomous system navigating such an environment, an important prerequisite for effective action decision making is information about the current state of the system. System states that are not known with a reasonable degree of certainty can be detrimental to successful mission completion. Self-localization typically involves using information received from the environment to determine position and orientation in a global frame [1], [2]. A possible approach to this self-localization process is to control or steer the vehicle in order to maximize the localization performance.

Localization algorithms are dependent on available sensors and measurable signals present in the environment. Common signal type/attributes used include: Time-Of-Arrival, Received Signal Strength, Angle-of-Arrival (AoA) [1]. These measurements are used to convey relative ranges and bearings between transmitter and receiver that the vehicle can use to determine location. AoA measurements can be determined by passive sensing, for example, using a camera and known landmark locations [3]. At least three AoA measurements are required to triangulate the position and orientation of an autonomous vehicle in a known environment where all systems are coplanar [4], [5] except when the vehicle is collinear with a vector connecting two transmitters and the vehicle and beacons lie on the circumference of a circle [6], [4]. For complete 2D localization, AoA measurements are more valuable than range measurements as they provide information on both position and orientation [7]. In real-world scenarios, the transmission of information is imperfect, and the measurements are often noisy. Noisy measurements can negatively impact the ability of the system to estimate position. In scenarios where the amount of noise effecting a measurement is spatially related to the transmitter and receiver, a vehicle should determine how to maneuverer to receive the best and most informative measurements. Related literature includes UAV path planning for localization of targets. A common performance index used in bearings-only target tracking literature is the determinant of the Fisher information matrix (FIM) [8], [9], [10], [11], [12]. In the case of self-localization, process noise affects the trajectory which is not taken into consideration when using the measurement FIM. Scalar measures based on the error covariance matrix such as trace and determinant are also used in target state estimation that inherently takes into account the stochastic nature of the process [13], [14], [15], [16]. These describe the mean square error, and volume of the error ellipsoid respectively, dependent on sensor measurement qualities and also sensor-target orientations [16]. The problem presented in this paper can be seen as the complementary problem to sensor path planning. Instead of several sensors moving to maximize target position localization, a single vehicle maneuvers around fixed transmitters to maximize its own estimation accuracy for both position and heading. The contribution of this paper is the development of a gradient descent based navigation algorithm for AoA self-localization. Also presented is a short discussion on the applicability of this method used in sensor path planning to a self-localization problem and suggestions for future work which could improve performance. This paper is organized as follows. In Section II, the localization problem is introduced. In Section III the optimal maneuvering methodology is presented, with detail on the steering algorithm used, constraints on the optimization problem and the cost function determined. Simulation results are displayed in Section IV, followed by a discussion of results in Section V and a conclusion is Section VI.

II. Problem Setup

A two-dimensional optimal maneuvering problem is considered, for a vehicle operating in an environment with $N \geq 1$ informative beacons. The N AoA measurements received from these beacons are used to estimate the vehicles position $(x_{v,k}, y_{v,k})$ and orientation (ϕ_k) at time k. The vehicle has

control over its rotational velocity and operates at a fixed linear speed. The following dynamic equation describes the state update of the system.

$$\begin{bmatrix} x_{v,k+1} \\ y_{v,k+1} \\ \phi_{k+1} \end{bmatrix} = \begin{bmatrix} x_{v,k} + TV\cos(\phi) \\ y_{v,k} + TV\sin(\phi) \\ \phi_k + T\omega_k \end{bmatrix} + \boldsymbol{w}_k, \tag{1}$$

The state vector for the vehicle dynamics is given by

$$\boldsymbol{x}_k = \begin{bmatrix} x_{v,k} & y_{v,k} & \phi_k \end{bmatrix}^T, \tag{2}$$

where $[x_{v,k}, y_{v,k}]^T$,$[\phi_k]$ are the vehicles position and heading respectively at time k. In (1), T is the constant time interval between the discrete time instances k; V is the vehicle velocity and ω is the rotational velocity at time k; $\boldsymbol{w}_k$ is the process noise and is modeled as a zero-mean Gaussian white noise with covariance $\mathbf{Q}_k$:

$$\boldsymbol{w}_k \sim \mathcal{N}(0, \mathbf{Q}_k). \tag{3}$$

The process noise accounts for unmodeled acceleration of the system state and has covariance matrix:

$$\mathbf{Q_k} = \begin{bmatrix} q_x\frac{T^2}{2} & 0 & 0 \\ 0 & q_y\frac{T^2}{2} & 0 \\ 0 & 0 & q_\phi\frac{T^2}{2} \end{bmatrix}. \tag{4}$$

For AoA localization, the non-linear measurement equation is

$$\boldsymbol{z}_k = \mathbf{h}(\boldsymbol{x}_k) + \boldsymbol{v}_k, \tag{5}$$

where $\boldsymbol{z}_k$ is a vector of *N* AoA measurements at time k, $\boldsymbol{v}_k$ is the measurement noise and is modeled as zero mean Gaussian white noise with covariance $\mathbf{R}_k(\boldsymbol{x}_k)$:

$$\boldsymbol{v}_k \sim \mathcal{N}(0, \mathbf{R}_k(\boldsymbol{x}_k)). \tag{6}$$

In terms of the vehicle states and beacon positions, the non-linear measurement function $\mathbf{h}$ becomes:

$$\mathbf{h}(\boldsymbol{x}_k) = \begin{bmatrix} \angle([x_{b1}, y_{b1}]^T - [x_{v,k}, y_{v,k}]^T) - \phi_k \\ \angle([x_{b2}, y_{b2}]^T - [x_{v,k}, y_{v,k}]^T) - \phi_k \\ \vdots \\ \angle([x_{bN}, y_{bN}]^T - [x_{v,k}, y_{v,k}]^T) - \phi_k \end{bmatrix}, \tag{7}$$

where $(x_{b,i}, y_{b,i})$ are the x and y position of the ith beacon and $\angle\boldsymbol{z}$ is the angle of a vector $\boldsymbol{z}$. The covariance matrix of the noise associated with the AoA measurements is assumed to take the following diagonal form.

$$\mathbf{R}_k(\boldsymbol{x}_k) = \begin{bmatrix} R_{k,1} & & 0 \\ & \ddots & \\ 0 & & R_{k,N} \end{bmatrix}, \tag{8}$$

where $R_{k,i} = \sigma_i^2 d_{k,i}^2 + \sigma_{i,min}^2$, σ_i^2 is the AoA signal noise variance for measurement i at unit range from the beacon and $\sigma_{i,min}^2$ is the floor noise variance for the sensor reading. $d_{k,i}$ is the distance between the vehicle and the i^{th} beacon. Due to the stochastic nature of the state transition and measurement equations, an estimator is employed to use the noisy measurements to produce a best estimate of the system states. The estimator needs to be compatible with nonlinear state transition and measurement functions and for this reason an extended Kalman filter (EKF) has been selected. The EKF utilizes a first order approximation of the Taylor series expansion for the non-linear state transition and measurement equations to arrive at a linear approximation that can be used in the covariance update equation. The traditional Kalman filter update equations can then be used with the approximate linear equations:

State Prediction:

$$\hat{\boldsymbol{x}}_{k|k-1} = \mathbf{f}(\hat{\boldsymbol{x}}_{k-1|k-1}, \boldsymbol{u}_k), \tag{9a}$$

$$\mathbf{P}_{k|k-1} = \mathbf{A}_k\mathbf{P}_{k-1|k-1}\mathbf{A}_k^T + \mathbf{Q}_k, \tag{9b}$$

State Update:

$$\hat{\boldsymbol{x}}_{k|k} = \hat{\boldsymbol{x}}_{k|k-1} + \mathbf{K}_k(\boldsymbol{z}_k - \mathbf{h}(\hat{\boldsymbol{x}}_{k|k-1})), \tag{9c}$$

$$\mathbf{P}_{k|k} = (\mathbf{I} - \mathbf{K}_k\mathbf{H}_k)\mathbf{P}_{k|k-1}, \tag{9d}$$

$$\mathbf{K}_k = \mathbf{P}_{k|k-1}\mathbf{H}_k^T(\mathbf{H}_k\mathbf{P}_{k|k-1}\mathbf{H}_k^T + \mathbf{R}_k)^{-1}, \tag{9e}$$

where $\hat{\boldsymbol{x}}_{k|k-1}$ is the *a priori* state estimate, an estimate of the states of the system at time *k* using all of the measurements up to time *k-1*. $\mathbf{f}$ is the nonlinear state transition function, $\boldsymbol{u}_k$ is the input vector $[V\ \omega_k]^T$, $\mathbf{P}_{k|k-1}$ is the *a priori* error covariance matrix for the *a priori* state estimate at time *k*. $\hat{\boldsymbol{x}}_{k|k}$ and $\mathbf{P}_{k|k}$ are the *a posteriori* state estimate and error covariance matrix respectively after filtering at time *k*. To utilize the Kalman filter equations, the measurement matrix $\mathbf{H}_k$ and state transition matrix $\mathbf{A}_k$ must be determined from the non-linear measurement and state transition equations (1) and (5). $\mathbf{A}_k$ is the 3×3 Jacobian matrix with respect to the system states evaluated at $\boldsymbol{x}_{k-1|k-1}$ and H_k is a N×3 Jacobian matrix of the measurement function $\mathbf{h}(x)$ evaluated at $\boldsymbol{x}_{k|k-1}$.

$$\mathbf{A}_k = \begin{bmatrix} 1 & 0 & -TV\sin(\phi_{k-1|k-1}) \\ 0 & 1 & TV\cos(\phi_{k-1|k-1}) \\ 0 & 0 & 1 \end{bmatrix}, \tag{10}$$

$$\mathbf{H}_k = \begin{bmatrix} \frac{d^y_{1,k|k-1}}{\|d_{1,k|k-1}\|^2} & \frac{-d^x_{1,k|k-1}}{\|d_{1,k|k-1}\|^2} & -1 \\ \frac{d^y_{2,k|k-1}}{\|d_{2,k|k-1}\|^2} & \frac{-d^x_{2,k|k-1}}{\|d_{2,k|k-1}\|^2} & -1 \\ & \vdots & \\ \frac{d^y_{N,k|k-1}}{\|d_{N,k|k-1}\|^2} & \frac{-d^x_{N,k|k-1}}{\|d_{N,k|k-1}\|^2} & -1 \end{bmatrix}, \tag{11}$$

where

$$d_{i,k|k-1} = \begin{bmatrix} d^x_{i,k|k-1} \\ d^y_{i,k|k-1} \end{bmatrix} = \begin{bmatrix} (x_{bi} - x_{v,k|k-1}) \\ (y_{bi} - y_{v,k|k-1}) \end{bmatrix}, i = 1, \ldots, N.$$

The recursive Kalman filter equations are initialized with

$$\boldsymbol{x}_0 = E\{\boldsymbol{x}_0\} \quad \text{and} \quad \mathbf{P}_0 = \mathrm{Cov}\{\boldsymbol{x}_0\}. \tag{12}$$

III. Optimal maneuvering

The objective of this optimal maneuvering algorithm is to provide a trajectory that will minimize the systems estimation error. Equivalently, the vehicle must maximize the information

it has about its position and heading. The control scheme consists of 2 parts, a navigation component which determines an optimal heading to minimize the cost function selected and a controller to determine a control input to achieve the desired trajectory. The vehicle must adhere to several constraints on its speed and position detailed in Section III-B. The rotational control of the vehicle is governed by the following linear state transition equation:

$$\phi_{k+1} = \phi_k + T\omega_k. \tag{13}$$

The control input is the rotational velocity ω_k. The cost function selected for the optimal control problem is introduced in Section III-C. The selected cost is minimized iteratively through a numerical gradient descent algorithm. At each time instant the gradient-descent algorithm determines a desired waypoint for the subsequent time instant. Following the path set by these iteratively selected points should result in the cost function reaching a minimum. The desired waypoint determined by the algorithm is then converted to a desired heading command ϕ_d. Finally a control input can be calculated to track the desired trajectory. The linear state update equation becomes:

$$\phi_{k+1} = \phi_k - TK(\phi_d - \phi_k), \tag{14}$$

where K is a gain used for the control.

A. Steering algorithm

The gradient descent algorithm uses the partial derivatives of the cost function with respect to changes in the x and y directions, to determine the optimal (x, y) waypoint at the next time step to minimize the cost function. Using this, a heading is calculated to maneuver the vehicle to this waypoint optimally. Eq. (15) details the desired state transition using the gradient descent algorithm:

$$\boldsymbol{x}_{d,k+1} = \begin{bmatrix} x_{d,k+1} \\ y_{d,k+1} \end{bmatrix} = \begin{bmatrix} \hat{x}_{v,k} \\ \hat{y}_{v,k} \end{bmatrix} - \mathbf{N}_k \frac{\partial J(\hat{\boldsymbol{x}}_k)}{\partial(\hat{x}_{v,k}, \hat{y}_{v,k})}, \tag{15}$$

where $\boldsymbol{x}_{d,k+1}$ is the desired waypoint at time $k+1$, $\hat{x}_{v,k}$ and $\hat{y}_{v,k}$ are the estimated x and y position of the vehicle at time k, $J(\boldsymbol{x}_k)$ is the cost function, $\mathbf{N}_k$ is a matrix for normalizing the gradient descent.

$$\mathbf{N}_k = \frac{VT}{\left\| \frac{\partial J}{\partial(\hat{x}_{v,k}, \hat{y}_{v,k})} \right\|} \mathbf{I}_2, \tag{16}$$

where $\mathbf{I}_2$ is the 2×2 identity matrix. The desired next point calculated with the gradient descent algorithm is used to determine the desired heading.

$$\phi_d = \operatorname{atan2}\left((x_{d,k+1} - \hat{y}_{v,k}), (y_{d,k+1} - \hat{x}_{v,k}) \right). \tag{17}$$

Opting for a numerical approximation of the gradient of $J(x_k)$, let

$$\frac{\partial J(\hat{\boldsymbol{x}}_k)}{\partial(\hat{x}_{v,k}, \hat{y}_{v,k})} = \begin{bmatrix} \alpha_k(1) & \alpha_k(2) \end{bmatrix}. \tag{18}$$

Using a first order approximation

$$\alpha_k(i) \approx \frac{J(\hat{\boldsymbol{x}}_k + \boldsymbol{\delta}_i) - J(\hat{\boldsymbol{x}}_k)}{\delta}, \tag{19}$$

where $\boldsymbol{\delta}_i$ is a 3×1 vector with zero entries except for the ith element which is small, real positive number δ, i.e.,

$$\boldsymbol{\delta}_1 = \begin{bmatrix} \delta & 0 & 0 \end{bmatrix}^T, \boldsymbol{\delta}_2 = \begin{bmatrix} 0 & \delta & 0 \end{bmatrix}^T. \tag{20}$$

B. Constraints

The vehicle is subject to several operational constraints on both its position and velocity. The velocity constraints are in the form of norm and turn rate constraints.

$$\left\| \begin{bmatrix} x_{v,k+1} - x_{v,k} \\ y_{v,k+1} - y_{v,k} \end{bmatrix} \right\| = VT, \tag{21a}$$

$$|\phi_{(k+1)} - \phi_k| \leq T\omega_{max}, \tag{21b}$$

where ω_{max} is the maximum turn rate of the vehicle. The hard constraints (21a) (21b) come from the physical limitations of the system, whereas the position constraints come from the nature of the problem. For an environment with N beacons, there are N soft position constraints of the form:

$$\left\| \begin{bmatrix} x_{v,(k+1)} - x_{b,i} \\ y_{v,(k+1)} - y_{b,i} \end{bmatrix} \right\| \geq d_{min}. \tag{22}$$

d_{min} is the minimum distance the vehicle can be positioned with respect to a beacon. These constraints correspond to a circle of radius d_{min} centered on each of the N beacons, in which the vehicle cannot travel within. In a planar environment the vehicle needs to maintain a distance from the transmitter, because if they are concurrent an angle between them cannot be measured. d_{min} should be larger than necessary to account for occasions when the vehicle can not avoid violating the constraint due to a limit on maximum turn rate. If the desired control input violates the maximum turn rate constraint, the control input is adjusted such that

$$|\phi_{(k+1)} - \phi_k| = T\omega_{max}. \tag{23}$$

The control input subject to constraints becomes:

$$\omega_k = \begin{cases} \frac{-\theta_{max}}{T}, & \text{for } -\theta_{max} < \theta_d - \phi_k \\ \frac{\theta_{max}}{T}, & \text{for } \theta_d - \phi_k > \theta_{max} \\ \frac{\theta_d - \phi_k}{T}, & \text{for } -\theta_{max} \leq \theta_d - \phi_k \leq \theta_{max} \end{cases} \tag{24}$$

where $\theta_{max} = T\omega_{max}$.

C. Cost function

To minimize estimation error variance for localization, it is important to maximize the amount of information the system has about itself. A cost function must be determined that when minimized will achieve this goal. We have decided to select the following cost function:

$$J_k = \det(P_{k+1|k\{1:2,1:2\}}). \tag{25}$$

Equation (25) is the determinant of the upper left portion of the *a priori* error covariance matrix, which corresponds to the area of the error ellipsoid of the position estimate. Minimizing this cost will lead the vehicle to a position where the error ellipsoid area is minimized which corresponds to a better state estimate.

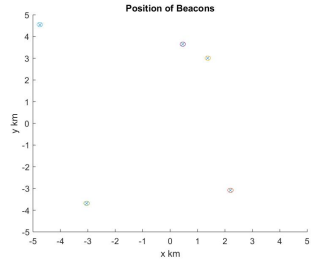

(a) Beacon Positions

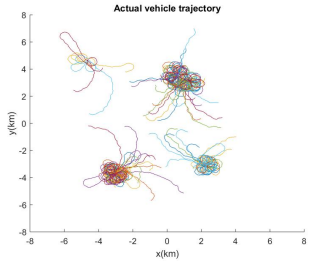

(b) Vehicle Trajectories for 50 runs

Fig. 1: Beacon positions and vehicle trajectories for randomly placed beacons

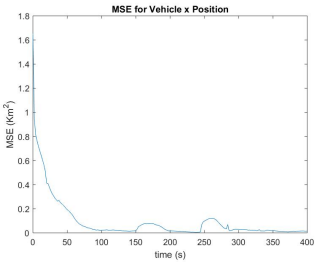

(a) MSE for Vehicle x Position

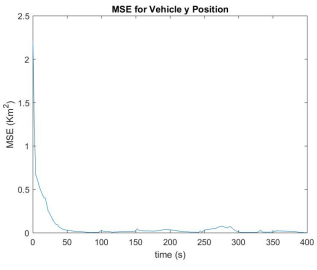

(b) MSE for Vehicle y Position

Fig. 2: MSE for vehicle position in 5 beacon environment

IV. Simulations

Simulations were run to evaluate the estimation performance and the effectiveness of the maneuvering strategy. Two different beacon geometries were investigated, five randomly distributed beacons and three equidistantly placed beacons. The parameters constant over all simulations are as follows: Let $\sigma_{r,i}$ be the standard deviation of AoA measurement noise from beacon i.

$$0.5001^\circ < \sigma_{r,i} < 1.5^\circ \text{ for } 0.1\text{km} < d_{k,i} < 10\text{km}, \qquad (26)$$

This corresponds to variances of $6.0923 \times 10^{-5} d_{k,i} + 7.6154 \times 10^{-5}$ radians. The initial covariance matrix $P_0 = \text{diag}(2.25, 2.25, 0.1745)$. V = 30m/s, ω_{max} = 0.1rad/s, T = 2s, simulation time = 400s, $\delta = 10^{-3}$km, d_{min} = 0.2km. The process noise is $q_x = q_y = q_{phi} = 10^{-4}$.

A. Randomly placed beacons

For the results displayed in this section, five beacons were randomly placed in a 5km×5km square centered at the origin. The x and y position of the beacons are:

$$\begin{bmatrix} x_{b,1} \dots x_{b,5} \\ y_{b,1} \dots y_{b,5} \end{bmatrix} = \begin{bmatrix} 2.200 & 1.374 & 0.461 & -3.042 & -4.749 \\ -3.084 & 3.005 & 3.649 & -3.685 & 4.552 \end{bmatrix}$$

The position of the beacons are displayed in Fig. 1a.

In the first simulation, the initial state estimate positioned the vehicle on the circumference of a circle with a 3km radius, centered at the origin. 50 simulations were executed at 50 equally spaced initial positions around the circle. The true inital state values were randomly distributed according to the initial covariance matrix P_0. Figure 1b show the actual trajectories, and Figures 2a and 2b display the MSE for these 50 runs.

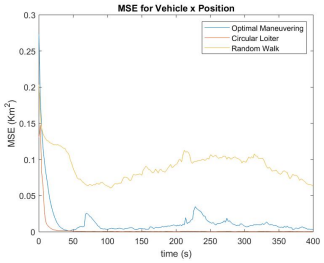

(a) MSE for x Position

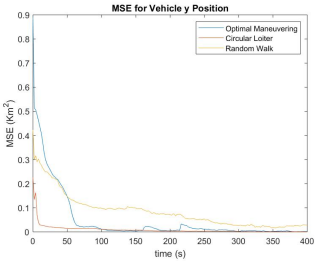

(b) MSE for y Position

Fig. 3: Comparison of position MSE for an optimally maneuvering vehicle, a loitering vehicle and a randomly walking vehicle, in a 5 beacon environment

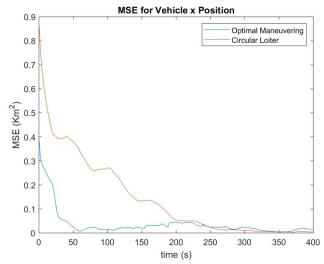

(a) MSE for x Position (P_0)

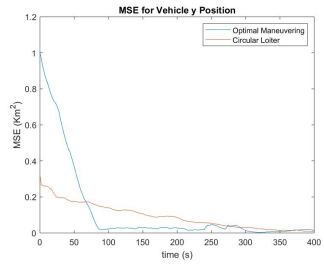

(b) MSE for y Position (P_0)

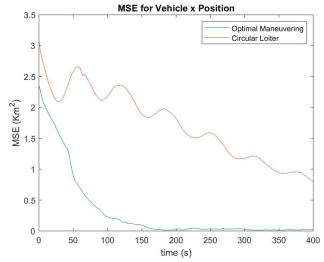

(c) MSE for x Position ($P1_0$)

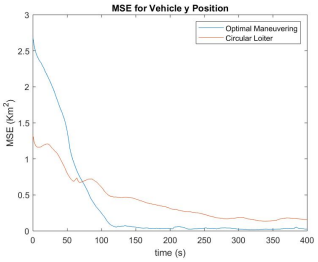

(d) MSE for y Position ($P1_0$)

Fig. 4: Comparison of position MSE for an optimally maneuvering vehicle and a loitering vehicle in a 3 beacon environment with different initial estimate error covariance matricies

A second simulation was run in the same environment, comparing a vehicle using the optimal maneuvering algorithm with a vehicle loitering around its initial position and a vehicle with randomized control input ω_k. In this simulation the mean of the initial state estimate was situated at the origin. Figures 3a and 3b show the MSE of the x and y position for a vehicle employing these steering algorithms.

B. Equidistant beacon geometries

From Section I, the minimum number of beacons to perform triangulation is three. In the following simulations, three beacons were placed equidistantly on the circumference of a

circle centered at the origin with a radius of 3km.

$$\begin{bmatrix} 0 & 3\cos(\frac{\pi}{6}) & -3\cos(\frac{\pi}{6}) \\ 3 & -3\sin(\frac{\pi}{6}) & -3\sin(\frac{\pi}{6}) \end{bmatrix} \tag{27}$$

Figures 4a and 4b show the MSE for 50 runs of both the vehicles performing optimal maneuvering, and vehicles loitering. Initial position state estimate has a mean at the origin, with initial covariance matrix P_0. Figures 4c and 4d show the MSE for 50 runs in the three beacon environment, except the initial estimate is more uncertain. In the simulation that produced these MSE plots, the initial position used was x_0 = $[0, 0, 0]^T$ + w_0 where $w_0 \sim \mathcal{N}(0, P1_0)$, $P1_0 = \mathrm{diag}(5, 5, 0.1745)$

V. Discussion

The optimal maneuvering scheme iteratively draws the vehicle towards a position which minimizes the area of the error ellipsoid for its position. As can be seen from observing Fig. 1b, this behavior drew the vehicle towards one of the beacons in the environment. The vehicles maneuvered towards a beacon, circling nearby while avoiding a violation of the proximity constraints surrounding the beacons. This result is interesting, as intuitively the center of the beacon field seems the most advantageous position to be. Circling the beacons expose the vehicle to geometrically undesirable estimation locations, which were not avoided because the inaccuracies are not captured in the error covariance matrix. The source seeking behavior as implemented achieves the minimum estimation variance as perceived by the EKF, but in reality is subject to undesirable errors. This is clear in Fig. 2a and 2b, where the loitering vehicles performed better in the dense beacon field, however the algorithm does perform better than randomly maneuvering. In the scenarios where three beacons were present, less information was available for self-localization and hence an information oriented navigation algorithm is desirable. In these scenarios the optimal maneuvering algorithm is in general, superior. Using the initial estimate covariance matrix $P0$, in Figures 4a and 4b the MSE converged faster at the expense of a higher MSE towards the end of the simulation time. The increased performance of the optimal maneuvering algorithm is more prominent when comparing Figures 4c and 4d when less initial information is present. The optimal maneuvering MSE for x and y converged much faster than for a loitering vehicle, in the time the simulations ran the MSE for the loitering vehicle did not converge.

VI. Conclusion

In this paper an optimal maneuvering methodology based on gradient descent is introduced that steers an autonomous vehicle to locations that provide better estimation accuracy. Initial results show that it performs well in environments with less available information, however in dense beacon fields its performance suffers due to unmodeled uncertainties. The algorithm successfully minimizes the selected cost function. The estimator gives a statistical best estimate of the vehicle states, however, it does not take into account sources of error that the Kalman filter can not model due to linearization, and unobservable beacon/vehicle geometries. In less informative environments the proposed algorithm leads to a faster convergence of MSE when compared to a loitering vehicle. Future work involves adding capability to distinguish uninformative maneuvers based on information that is not statistically derived but semantic in nature. Information that is derived from the states of the vehicle/environment system. This additional information could help minimize estimation errors that arise from large errors in initialization, allowing for faster convergence in these scenarios. Other more complex scenarios should be investigated including when beacons can move dynamically, when positions are not known and when the vehicle is balancing optimization criteria for gathering information and achieving a primary objective.

References

[1] N. Bulusu, J. Heidemann, and D. Estrin, "GPS-less low-cost outdoor localization for very small devices," *IEEE personal communications*, vol. 7, no. 5, pp. 28–34, 2000.

[2] K. Dogancay, "Exploiting geometric translations in tls based robot localization from landmark bearings," in *2009 17th European Signal Processing Conference*, Aug 2009, pp. 95–99.

[3] I. Loevsky and I. Shimshoni, "Reliable and efficient landmark-based localization for mobile robots," *Robotics and Autonomous Systems*, vol. 58, no. 5, pp. 520–528, 2010.

[4] J. S. Esteves, A. Carvalho, and C. Couto, "Generalized geometric triangulation algorithm for mobile robot absolute self-localization," in *Industrial Electronics, 2003. ISIE'03. 2003 IEEE International Symposium on*, vol. 1. IEEE, 2003, pp. 346–351.

[5] K. Dogancay, "Self-localization from landmark bearings using pseudolinear estimation techniques," *IEEE Transactions on Aerospace and Electronic Systems*, vol. 50, no. 3, pp. 2361–2368, July 2014.

[6] M. Betke and L. Gurvits, "Mobile robot localization using landmarks," *IEEE transactions on robotics and automation*, vol. 13, no. 2, pp. 251–263, 1997.

[7] D. Niculescu and B. Nath, "Ad hoc positioning system (APS) using AOA," in *INFOCOM 2003. Twenty-Second Annual Joint Conference of the IEEE Computer and Communications. IEEE Societies*, vol. 3. Ieee, 2003, pp. 1734–1743.

[8] J. E. L. Cadre and C. Jauffret, "Discrete-time observability and estimability analysis for bearings-only target motion analysis," *IEEE Transactions on Aerospace and Electronic Systems*, vol. 33, no. 1, pp. 178–201, Jan 1997.

[9] J.-M. Passerieux and D. Van Cappel, "Optimal observer maneuver for bearings-only tracking," *IEEE Transactions on Aerospace and Electronic Systems*, vol. 34, no. 3, pp. 777–788, 1998.

[10] A. N. Bishop and P. N. Pathirana, "Optimal trajectories for homing navigation with bearing measurements," *IFAC Proceedings Volumes*, vol. 41, no. 2, pp. 12 117–12 123, 2008.

[11] S. Hammel, P. Liu, E. Hilliard, and K. Gong, "Optimal observer motion for localization with bearing measurements," *Computers & Mathematics with Applications*, vol. 18, no. 1-3, pp. 171–180, 1989.

[12] Y. Oshman and P. Davidson, "Optimization of observer trajectories for bearings-only target localization," *IEEE Transactions on Aerospace and Electronic Systems*, vol. 35, no. 3, pp. 892–902, 1999.

[13] K. Dogancay, "Single-and multi-platform constrained sensor path optimization for angle-of-arrival target tracking," in *Signal Processing Conference, 2010 18th European*. IEEE, 2010, pp. 835–839.

[14] C. Leung, S. Huang, N. Kwok, and G. Dissanayake, "Planning under uncertainty using model predictive control for information gathering," *Robotics and Autonomous Systems*, vol. 54, no. 11, pp. 898–910, 2006.

[15] K. Dogancay, "UAV path planning for passive emitter localization," *IEEE Transactions on Aerospace and Electronic Systems*, vol. 48, no. 2, pp. 1150–1166, APRIL 2012.

[16] C. Yang, L. Kaplan, and E. Blasch, "Performance measures of covariance and information matrices in resource management for target state estimation," *IEEE Transactions on Aerospace and Electronic Systems*, vol. 48, no. 3, pp. 2594–2613, 2012.